Molecular Crystals and Liquid Crystals

ISSN: 1542-1406 (Print) 1563-5287 (Online) Journal homepage: http://www.tandfonline.com/loi/gmcl20

Fluorescence and amplified emission properties of single-crystal 2,5-bis(4-biphenylyl)thiophene

Yasuyuki Ono, Fumio Sasaki & Hisao Yanagi

To cite this article: Yasuyuki Ono, Fumio Sasaki & Hisao Yanagi (2016) Fluorescence and amplified emission properties of single-crystal 2,5-bis(4-biphenylyl)thiophene, Molecular Crystals and Liquid Crystals, 629:1, 229-234, DOI: 10.1080/15421406.2015.1096436

To link to this article: http://dx.doi.org/10.1080/15421406.2015.1096436

Published online: 16 Jun 2016.

MOLECULAR CRYSTALS AND LIQUID CRYSTALS
2016, VOL. 629, 229–234
http://dx.doi.org/10.1080/15421406.2015.1096436

Taylor & Francis
Taylor & Francis Group

Fluorescence and amplified emission properties of single-crystal 2,5-bis(4-biphenylyl)thiophene

Yasuyuki Ono[a], Fumio Sasaki[b], and Hisao Yanagi[a]

[a]Graduate School of Materials Science, Nara Institute of Science and Technology (NAIST), Ikoma, Nara (Japan); [b]Electronics and Photonics Research Institute, National Institute of Advanced Industrial Science and Technology (AIST), Tsukuba, Ibaraki (Japan)

ABSTRACT

Ligth amplification properties are investigated for single crystals of commercially available 2,5-bis(4-biphenylyl)thiophene. Depending on growth methods, three kinds of crystals are obtained having different fluorescence spectra in blue-green color. Under optical pumping, their amplified spontaneous emission (ASE) bands appear at different wavelengths. The solution-grown crystal shows ASE bands at $\lambda = 464$ and 494 nm which are assigned to the 0–1 and 0–2 transitions, respectively. By contrast, the vapor- and slide-boat-grown crystals show a red-shifted 0–1 band at $\lambda = 496$ and a 0–2 band at 520 nm, respectively.

KEYWORDS

2,5-bis(4-biphenylyl)thiophene; single crystal; fluorescence; amplified spontaneous emission; organic laser

Introduction

The recent successful development of organic light-emitting diodes (OLEDs) envisages us to realize electically pumped organic lasers [1–3]. Among various issues required for organic lasing, materials robustness has to be first considered. As a prerequisite investigation, optically pumped light amplification and lasing have been extensively studied for a variety of materials [4,5]. Amplified spontaneous emission (ASE) is a primary measure wether the material has a potential as a lasing medium. For effective amplification, the orientation of emitting molecules in lasing media plays an significant role since the stimulated emission is enhanced among transition dipole moments aligning in parallel [6]. Therefore, a crystalline medium having thin molphology with appropriate molecular orientation is a good candidate of organic lasing at lower excitation threshold [7,8].

To meet those requirements, we choose thiophene/phenylene co-oligomers (TPCOs) which are linearly π-conjugated molecules with arbitrary numbers and sequences of thiophene and phenylene units [9,10]. Most of TPCOs are crystallized in thin platelet morplology in which the chain-like molecules are assembled with suitable uniaxial orientation [11]. Since the π-π^* transition dipole moment between the highest occupied molecular orbital (HOMO) and the lowest unoccupied one (LUMO) is parallel to the oligomer axis, the standing orientation against the crystal plane promotes light confinement within the crystal slab and propagation of fluorescence by the transverse magnetic (TM) mode [12]. This linearly polarized

CONTACT Yasuyuki Ono yanagi@ms.naist.jp
Color versions of one or more of the figures in the article can be found online at www.tandfonline.com/gmcl.
This paper was originally submitted to *Molecular Crystals and Liquid Crystals,* Volumes 620–622, Proceedings of the KJF International Conference on Organic Materials for Electronics and Photonics 2014.

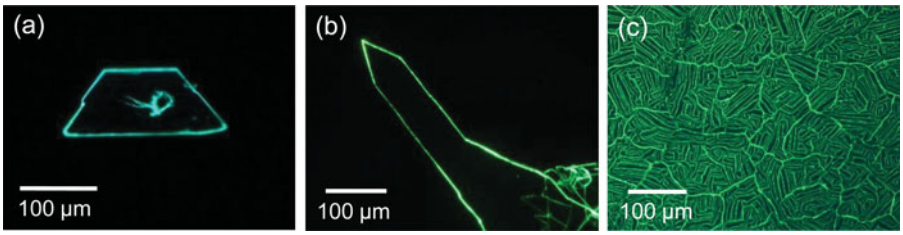

Figure 1. Fluorescence micrographs of BP1T crystals prepared by solution (a), vapor (b) and slide-boat (c) growth.

propagation effectively enhances the stimulated emission under optical pumping conditions resulting in ASE radiation from the crystal edges. Moreover, well-grown facets at the parallel side-edges can act as a Fabry–Pérot (F-P) mirror resulting in laser oscillations [13–15].

Such ASE and lasing performances are dependent upon spectral characteristics as well as a quality of the TPCO crystals. In this study, we found that such spectral characteristics are remarkably varied by growth methods of TPCO crystals. Three kinds of crystals with different fluorescence colors are prepared by solution, vapor and slide-boat growth using commercially available 2,5-bis(4-biphenylyl)thiophene (BP1T).

Experimental

A BP1T sample was purchased from Tokyo Chemical Industry Co., Ltd. and used after purification by sublimation at 300°C in an evacuated tuve oven (5 kPa). Then, three kinds of crystal growth were performed according to the following procedures. For solution growth, 10 mg of BP1T was dissolved in 20 ml 1,2,4-trichlorobenzene by heating at 180°C. The solution was slowly cooled down to 40°C at a rate of ~12°C/hr to precipitate thin platelet crystals. Vapor growth was carried out by heating the sample powder at 300°C for 3 hr in a glass tube with a nitrogen flow at 10 ml/min. After cooled to 30°C in 6 hr, thin flake-like crystals grew sticking on the glass tube wall due to temperature gradient in a tube oven. Those solution- and vapor-grown crystals were transferred onto a glass substrate (10×10 mm^2) by using a tungsten tip and provided for optical measurements. Polycrystalline films were obtained directly on a glass substrate by a slide-boat method [16]. The BP1T sample was provided from a bottom slit of a stainless crucible heated at 285°C in air while the glass substrate kept at 220°C in contact with the bottom slit was laterally moved at a speed of 170 μm/s.

Morphology of obtained crystals was observed with a fluorescence microscope (Olympus BX-51) under ultraviolet excitation ($\lambda_{ex} = 365$ nm). Photoluminescence (PL) measurements were performed with a excitation source of second harmonics from a Ti:S femtosecond pulsed laser ($\lambda = 397$ nm, 1 kHz, 200 fs duratione). The excitation light shaped in a rectangle of 33 $\times$ 160 μm^2 was incident with p-polarization at an angle of 20° against the crystal plane. The emitted light was collected in the direction parallel to the crystal plane with a CCD spectrometer (Roper Scientific ST-133 series).

Results and discussion

Depending upon growth methods, the obtained BP1T crystals exhibit diffrent morphology and fluorescence color as shown in fluorescence micrographs in Fig. 1. The solution-grown crystal forms a thin platelet with a polygonal shape. As seen in Fig. 1(a), bluish fluorescence is remarkably observed at the crystal edges besides a defect on the crystal plane. It suggests that

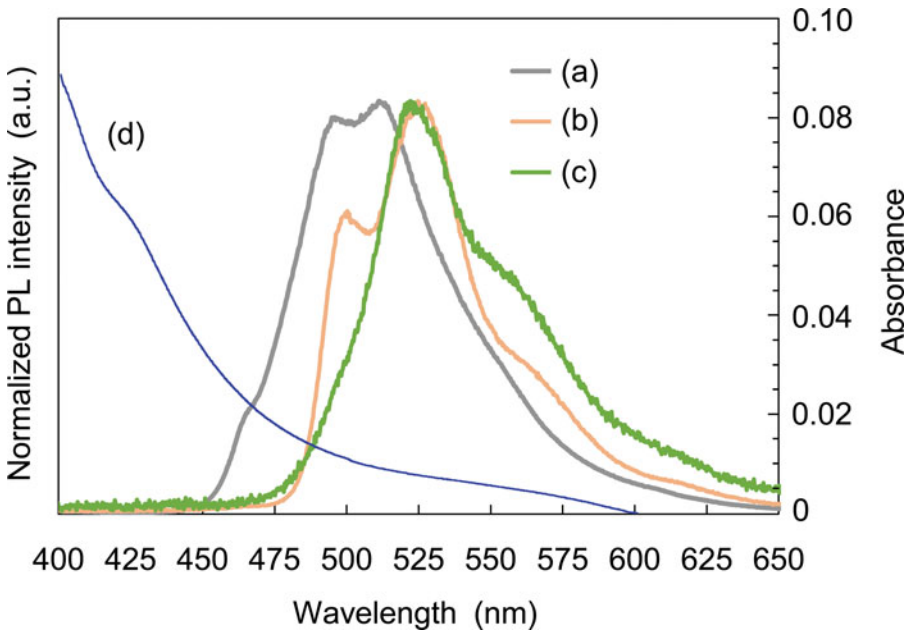

Figure 2. Fluorescence spectra taken from BP1T crystals prepared by solution (a), vapor (b) and slide-boat (c) growth. Absorption spectrum of a vapor-deposited BP1T film (d).

the emitted light is confined within the crystal slab and waveguided along its plane. This confined light propagation is supported by standing orientation of molecular axes almost upright against the crystal *ab*-plane [17]. Therefore, PL spectra were collected from the platelet edge along a direction parrallel to the crystal plane. A fluorescence spectrum of this solution-grown crystal taken at weak excitaion fluence is shown in Fig. 2(a). A shoulder at 465 nm and a peak at 495 nm are assigned to vibronic progressions of 0–1 and 0–2 transitions, respectively, according to the reported spectra obtained for a single-crystal BP1T synthesized by S. Hotta [8,12]. However, another peak around at 515 nm, which can not be assigned to a vibronic progression of 0–3, and a long-wavelength tail over 550 nm have never been found for previously reported BP1T crystals.

The vapor and slide-boat growth yielded crystals showing green fluorescence being different from the solution growth. The vapor-grown crystal is obtained in a thin flake sometimes partly having a regular platelet as shown in Fig. 1(b). The fluorescence spectrum of this crystal shows red-shifted progressions at 500, 525 and 560 nm as shown in Fig. 2(b). In contrast to free-standing crystals obtained by those solution- and vapor-growths, the slide-boat growth resulted in a polycrystalline film composed of single-crystal grains in size of $\sim$100 μm as seen in Fig. 1(c). The green fluorescence is scattered at the grain boundaries as well as at cracks formed in the cooling process which are caused by difference in thermal shrinkage between the BP1T crystal and glass substrate. Assignment of fluorescence bands shown in Fig. 2(c) are identical to those of the vapor-grown crystal although the peak at 500 nm is decreased while the shoulder at 560 nm is increased. This difference in the peak intensity is attributed to self-absorption effect. As shown in the absorption spectrum of a BP1T film (Fig. 2(d)), the fluorescence light collected along the direction parallel to the substrate/crystal plane suffers from scattering and absorption during long propagation in the polycrystalline film resulting in quenching of the shorter-wavelength emission.

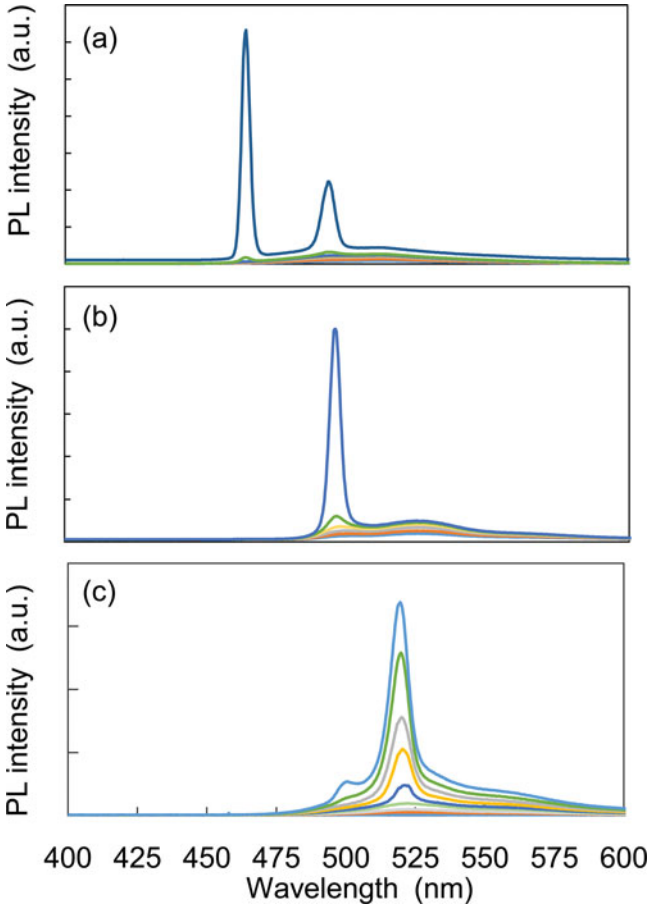

Figure 3. Excitation density dependences of PL spectra taken from BP1T crystals prepared by solution (a), vapor (b) and slide-boat (c) growth.

We next investigated light amplification properties of those three kinds of BP1T crystals. Figure 3 shows their excitation-density dependences of PL spectra taken with increasing optical pumping power. In the measurements for the solution- and vapor-grown crystals, the excitation beam is incident to the crystal surface such that the longer axis of the rectangle beam ($33 \times 160\ \mu m^2$) is parpendiclar to the parallel pair of side facets. When the excitation-density is beyond 500 $\mu J/cm^2$, the solution-grown blue crystal shows gain-narrowed ASE peaks at $\lambda = 464$ and 494 nm which emerges from the 0–1 and 0–2 fluorescence bands, respectively (Fig. 3(a)). This ASE appearance is similar to that previously reported for the BP1T crystal [8] although the fluorescence intensity of the 0–1 band (Fig. 2(a)) is considerably weaker than that of the previously reported one. By contrast, the vapor-grown green crystal exhibits one ASE peak at $\lambda = 496$ nm (Fig. 3(b)) which corresponds to the red-shifted 0–1 florescence band (Fig. 2(b)). On the other hand, the ASE peak of slide-boat-grown crystal emerges at $\lambda = 520$ nm in the 0–2 fluorescence band (Fig. 3(c)) due to its increased intensity relative to the 0–1 band (Fig. 2(c)).

In Fig. 4, the excitation-density dependences of those ASE intensities are compared for three crystals. The integrated intensity of the 0–1 band ($\lambda = 464$ nm) for the solution-grown crystal nonlinearly increased when the excitation density is beyond an ASE threshold of

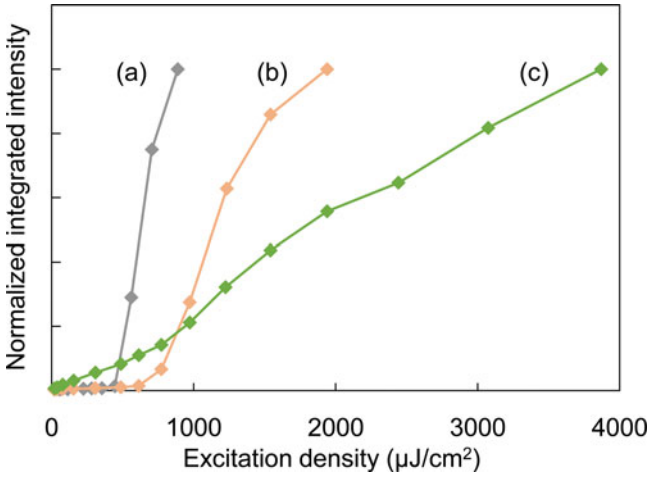

Figure 4. Integrated intensities of PL bands plotted as a function of excitation density for BP1T crystals prepared by solution (a), vapor (b) and slide-boat (c) growth. The PL intensity was integrated at the 0–1 bands in (a) and (b), and at the 0–2 band in (c).

445 μJ/cm^2. The vapor-grown crystal also shows a similar nonliner amplification of the 0–1 band ($\lambda = 496$nm), however, the ASE threshold is increased to 613 μJ/cm^2 and its slope factor is decreased. This deteoriated propertiy is ascribed to irregular morphology of the vapor-grown crystal (Fig. 1(b)) as compared to the polygonal shape of the solution-grown crystal (Fig. 1(a)). In the vapor-grown crystal, a portion of light emitted at its sword-like part is difussed to the thin flake body which does not contribute to the stimulated emition process. On the other hand, the emitted light is effctively confined inside the solution-grown crystal since the polygonal side facets function as feed-back mirrors. In fact, a high-resolution spectrum taken from the solution-grown crystal exhibits laser oscilations on an spectral envelope of the 0–1 and 0–2 ASE bands as shown in Fig. 5. According to the relation, $n_g = 1/2L\Delta\nu$ (n_g: group index, L: cavity length, $\Delta\nu$: mode interval), refractive indices of $n_g = 6.0$ and 4.5 were obtained at the ASE peak wavelengths of the 0–1 and 0–2 bands, respectively. These high n_g values supports effective light confinement in the BP1T crystal. In contrast to the solution- and vapor-grown crystals, the excitation-density dependence of the slide-boat-grown crystal

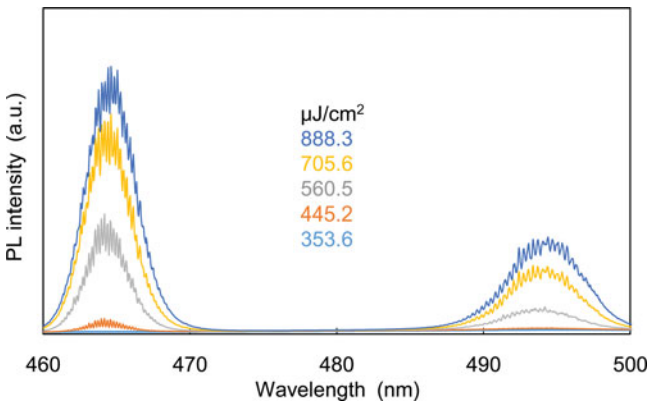

Figure 5. Excitation density dependences of high-resolution PL spectra taken from solution-grown BP1T crystal.

shows less remarkable nonlinear increase of its 0–2 band intensity ($\lambda = 520$ nm). Light scattering at the grain boundaries and fine cracks (Fig. 1(c)) limits the confined propagation of emitted light resulting in a higher threshold of 772 μJ/cm^2 and a lower slope factor.

The reason for their spectral changes depending on the growth methods is still open question. In order to clarify possible red-shift mecanisms such as energy-transfer to impurity species and modification of molecular packing, we are now under investigation by means of x-ray diffraction, elemental analysis and mass spectroscopy.

Conclusions

In this study, three kinds of crystal growth methods were applied to a commercially available BP1T which is one of extensively studied materials for organic laser. The morphology and fluorescence color of the obtained crystals were varied depending on different temperature and atomosphere in the solution-, vapor- and slide-boat growth. Consequently, amplified emission was obtained for all crystals at different wavelengths according to their red-shifted fluorescence spectra.

Acknowledgments

This work was supported by Grant-in-Aid for Scientific Research (B) No. 25286042 from Japan Society for the Promotion of Science (JSPS) and the Green Photonics project of Nara Institute of Science and Technology.

References

[1] Tessler, N. (1999). *Adv. Mater.*, *11*, 363.
[2] Samuel, I. D. W., Namdas, E. B., & Turnbull, G. A. (2009). *Nat. Photonics*, *3*, 546.
[3] Liu, X., Li, H., Song, C., Liao, Y., & Tian, M. (2009). *Opt. Lett.*, *34*, 503.
[4] Hide, F., Díaz-Gracía, M. A., Schwartz, B. J., Andersson, M. R., Pei, Q. & Heeger, A. J. (1996). *Science*, *273*, 1833.
[5] Tessler, N., Denton, G. J., Friend, R. H., & Forrest, S. R. (1996). *Nature*, *383*, 695.
[6] Yanagi, H., Ohara, T., & Morikawa, T. (2001). *Adv. Mater.*, *13*, 1452.
[7] Fichou, D., Delysse, S., & Nunzi, J.-M. (1997). *Adv. Mater.*, *9*, 1778.
[8] Nagawa, M., Hibino, R., Hotta, S., Yanagi, H., Ichikawa, M., Koyama, T., & Taniguchi, Y. (2002) *Appl. Phys. Lett.*, *80*, 544.
[9] Hotta, S., Lee, S. A., & Tamaki, T. (2000). *J. Heterocycl. Chem.*, *37*, 25.
[10] Hotta, S., Kimura, H., Lee, S. A., & Tamaki, T. (2000). *J. Heterocycl. Chem.*, *37*, 281.
[11] Hotta, S., Goto, M., Azumi, R., Inoue, M., Ichikawa, M., & Taniguchi, Y. (2004). *Chem. Mater.*, *16*, 237.
[12] Yanagi, H., Sakata, I., Yoshiki, A., Hotta, S., & Kobayashi, S. (2006). *Jpn. J. Appl. Phys.*, *45*, 483.
[13] Ichikawa, M., Hibino, R., Inoue, M., Haritani, T., Hotta, S., Araki, K., Koyama, T., & Taniguchi, Y. (2005). *Adv. Mater. 17*, 2073.
[14] Yamao, T., Yamamoto, K., Taniguchi, Y., Miki, T., & Hotta, S. (2008). *J. Appl. Phys. 103*, 093115.
[15] Mizuno, M., Haku, U, Marutani, Y., Ishizumi, A., Yanagi, H., Sasaki, F., & Hotta, S. (2012). *Adv. Mater.*, *24*, 5744.
[16] Sasaki, F., Mochizuki, H., Yanagi, H., & Hotta, S. (2014). *Reports on the 468th topical meeting of the laser society of Japan*, No. RTM-14–48.
[17] Hotta, S., & Goto, M. (2002). *Adv. Mater. 14*, 498.